

Optimum structure with homogeneous optimum cellular material for maximum fundamental frequency

Bin Niu · Jun Yan · Gengdong Cheng

Received: 11 June 2008 / Revised: 18 October 2008 / Accepted: 19 October 2008 / Published online: 20 November 2008
© Springer-Verlag 2008

Abstract Ultra-light cellular materials exhibit high stiffness/strength to weight ratios and bring opportunity for multifunctional performance. One of their potential applications is to build structure with optimum dynamic performance, which is extremely important for some structural parts in vehicle engineering and attracts a great attention. This paper presents a two-scale optimization method and aims at finding optimal configurations of macro structures and micro-structures of cellular material with maximum structural fundamental frequency. In this method macro and micro densities are introduced as independent design variables for macrostructure and microstructure. Optimizations at two scales are integrated into one system through homogenization theory and base material is distributed between the two scales automatically with optimization model. Microstructure of materials is assumed to be homogeneous at the macro scale to meet today's manufacture practice and reduce manufacturing cost. Plane structure with homogeneous cellular material and perforated plate are studied. Numerical experiments validate the proposed method and computational model.

Keywords Two-scale topology optimization · Eigenfrequency design · Ultralight material · Homogenization

1 Introduction

With the development of engineering practice, the demand for high performance material is beyond traditional solid metal material. People expect new material possessing properties such as lightweight, high efficiency and multifunction. In order to realize this goal, various ultra-light materials including foam (Ashby et al. 2000), truss-like material (Wallach and Gibson 2001; Deshpande et al. 2001) and linear cellular material (Hayes et al. 2004) are developed and fabricated through controlling the geometry of material microstructures. These ultra-light materials have been widely used to construct light weight sandwich panel structures, for heat dissipation, vibration control and/or acoustic damping because of their relatively high stiffness/strength–weight ratios and tremendous opportunity for multifunctional applications.

The ultra-light materials can be divided into two groups. The first one is represented by foam material that has intrinsic microscopic randomness in microstructures. Because of the uncontrollable randomness the foam material is not a good choice for load-carrying structural components. Another group, including truss-like material and linear cellular material as shown in Fig. 1, differentiates itself by microstructures distributed periodically in space. The latter ones also have two additional advantages, namely their nearly perfect periodicity and high designability.

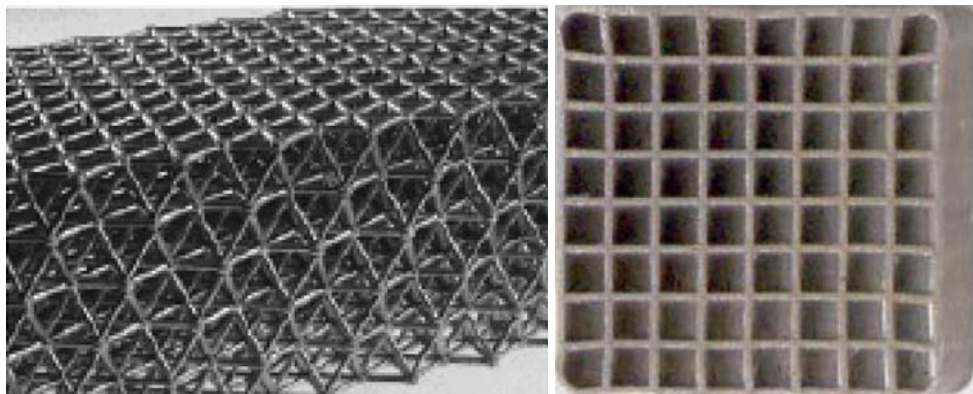
B. Niu · J. Yan · G. Cheng (✉)
State Key Laboratory of Structural Analysis for Industrial
Equipment, Department of Engineering Mechanics,
Dalian University of Technology,
Dalian 116024, People's Republic of China
e-mail: chenggd@dlut.edu.cn

B. Niu
e-mail: binniu@dl.cn

J. Yan
e-mail: yanjun@dlut.edu.cn

Fig. 1 Two representations of ultra-light materials.

- a** Truss-like material (Deshpande et al. 2001).
b Linear cellular material (Hayes et al. 2004)



Truss-like material (Deshpande et al. 2001)

Linear cellular material (Hayes et al. 2004)

The increasing recognition of this designability and the rapid developments in fabrication technique (Kooistra et al. 2004; Brittain et al. 2001; Cochran et al. 2002) have attracted more attention to design macrostructures composed of the periodic porous anisotropic materials or cellular materials. In this paper we focus mainly on macro plane structure with homogeneous cellular material. Another important ultra-light structure is perforated plate, which is formed by planar periodic repetition of a uniform 3D microstructure, but the microstructure doesn't vary along the plate thickness direction. Since the dynamic analysis and optimum design of perforated plate structure with cellular material follow the same approach, our study will cover perforated plate as well.

Although there are abundant studies on the elastic behavior of cellular materials under static loads, the dynamics of this class of cellular solids receives more attention recently. Wang and Stronge (1999) studied dynamic behavior of elastic regular hexagonal honeycombs under harmonically exciting forces using the micropolar theory. The effect of impact and energy absorption of metal honeycombs is studied by Evans et al. (2001), Xue and Hutchinson (2003). Banerjee and Bhaskar (2005) investigated the free vibration of elastic structures made up of cellular material through an approximate method. To the best of our knowledge, few work so far has been reported on two-scale concurrent optimum topology design of cellular materials considering vibration. Since structures made of these materials are frequently used under dynamic environments, there is a need to understand and optimize their dynamic behavior. The present study is motivated by this need. Structural topology optimization approach is utilized as a key tool.

When such a periodic material is used for constructing the macro structure that has the characteristic dimension much larger than the characteristic length of

the material microstructure, the periodic material can be homogenized for the reason of a more efficient analysis. This is a two-scale computing problem described by same continuum equations at macro and micro scales (Borst 2008). First, effective elastic properties of homogenized material are determined by an equivalence of the mechanical behavior of the representative microstructure. Then the computation at the macro scale can be implemented based on the effective properties. A variety of methods including analytical, numerical and experimental methods have been developed to calculate the effective mechanical properties, e.g. in the book (Gibson and Ashby 1997) and a recent review (Hohe and Becker 2002). As one of these methods, the mathematical homogenization method based on two-scale asymptotic expansion is widely applied in predicting the effective properties of periodic materials because of its rigorous mathematical foundation (see, e.g., Benssousan et al. 1978; Sanchez-Palencia 1980; Hassani and Hinton 1998). Perforated plate can be solved based on mathematical homogenization method in a similar way (Artola and Duvaut 1977; Liu et al. 1998; Bendsøe and Sigmund 2003, references therein).

Structural topology optimization aims at finding optimum topology to minimize structural weight or maximize structural performance under a given set of constraints. Different from size or shape optimization, structural topology optimization can achieve more efficient conception/configuration design in the stage of initial design, and it is a hot topic in recent two decades. The pioneering work of modern structural topology optimization can be traced back to 1981, when Cheng and Olhoff (1981) introduced the concept of microstructure to structural optimization in studying the optimum thickness design of a solid elastic plate for minimum compliance. The connection between shape optimization and homogenization of microstructured materials is discussed in a series of works on optimal design

problems introducing microstructures (see, e.g., Allaire 2002; Cherkaev 2000; Tartar 2000, for an overview). In 1988, Bendsøe and Kikuchi (1988) implemented the topology optimization via a homogenization method and lay a foundation of modern structural topology optimization. Later, SIMP (Solid Isotropic Material with Penalization) method by Bendsøe (1989) and Rozvany et al. (1992) was developed and used to implement topology optimization. ESO (Evolutionary Structural Optimization) (Xie and Steven 1993) and Level Set approach (Allaire et al. 2002; Wang et al. 2003) are two alternative topology optimization approaches. For the state of art in topology optimization reader is referred to the review (Eschenauer and Olhoff 2001) and the book (Bendsøe and Sigmund 2003).

Topology optimization with respect to structural vibration frequency was first considered by Diaz and Kikuchi (1992), who dealt with a single eigenvalue optimization problem. Subsequently, many works have been seen to extend topology optimization in dynamic problems (e.g., Ma et al. 1995; Krog and Olhoff 1999; Allaire et al. 2001; Allaire and Jouve 2005, etc.). Recently Jensen and Pedersen (2006) dealt with maximal eigenfrequency separation in two-material structures. Du and Olhoff (2007) discussed different approaches for topology optimization of vibrating structure. Topology optimization used to design periodic material with phononic band gaps is reported by Sigmund and Jensen (2003) and many others.

The present work is an attempt to achieve optimal structure composed of ultra-light materials by utilizing topology optimization at both structural and material scales. It aims at finding optimal configurations of the macro structure and material microstructure for maximizing fundamental frequency with specific base material amount. Microstructure of materials is assumed to be homogeneous at the macro scale to meet today's manufacture practice and reduce manufacturing cost. The two-scale structure and material analysis is performed based on the assumption that macroscopically cellular structures behave as a homogeneous continuum for low frequency dynamics instead of discrete complete cellular structures, which needs computationally expensive dynamic analysis. Plane structures and perforated plates are studied. In the optimization formulation, macro and micro densities are introduced as the design variables for the macro structure and material microstructure independently. The design of material microstructure is concurrently optimized with the structural topology design at the macro scale. Penalization approaches are adopted at both scales to ensure clear topologies, i.e. SIMP (Bendsøe 1989; Rozvany et al. 1992) at micro-scale and PAMP (Porous

Anisotropic Material Penalization) (Liu et al. 2008) at macro-scale. Optimizations at two scales are integrated into one system with homogenization theory and the distribution of base material between two scales can be determined automatically by the optimization model. The proposed method and computational model are validated by a number of numerical examples.

The organization of the rest of this paper is as follows. The two-scale design model for structure with homogeneous cellular material is described in Section 2. Two class design variables, namely macro density and micro density, are independently defined. Section 3 presents formulations of two-scale design optimization for maximum structural fundamental eigenfrequency. Penalization method for topology optimization of vibrating structures at two scales is given in Section 4. Section 5 gives briefly the formulation for vibration of perforated plate. Section 6 outlines various numerical examples in order to validate the proposed method, including plane and perforated plate problems. Finally, a summary of our observations and a conclusion close the paper. Appendix deals with the structural analysis and sensitivity analysis required for numerical optimization algorithms.

2 Two-scale design model for structure with homogeneous cellular material

Design of structure with homogeneous cellular material can be divided into two scales, i.e. design of structure at macro scale and material microstructure at micro scale. Many research works (Hyun and Torquato 2002; Sigmund 1995; Yan et al. 2006; Lipperman et al. 2008) for ultra-light materials aim at developing materials with prescribed or extreme properties, i.e. optimizing material microstructure in terms of certain homogeneous effective properties. Such optimum material is not guaranteed to be the most efficient when constructing structures, since both structural configuration and boundary conditions for different structures may vary dramatically in practical use. Rodrigues et al. (2002) proposed a hierarchical structure and material design method to achieve minimum system compliance. In this method macro design variable in every point equals the integral of micro design variables in the domain of microstructure corresponding to that point at macro scale. Furthermore, in this method microstructural configurations vary from point to point at the macro-scale, which results in a “varying gray” look of the structural design. Such results provide ideally optimum design, but may bring about an insurmountable manufacturing difficulty.

To be different from the both methods above, we proposed a two-scale optimization method to realize the topology optimization at two scales and find optimal topology of macro-structure and optimal configuration of micro-structure simultaneously. The basic idea of the method was presented in the paper (Liu et al. 2008). In this two-scale optimization method, macro and micro densities are introduced as independent design variables for macro structure and material microstructure, respectively. Optimizations at two scales are integrated into one system with homogenization theory and solved simultaneously without iterations between two scales. The optimal configurations at two scales can be decided automatically by the two-scale optimization model. Penalization approaches are adopted at both scales to ensure clear topologies, i.e. SIMP (Solid Isotropic Material Penalization) (Bendsøe 1989; Rozvany et al. 1992) at the micro-scale and PAMP (Porous Anisotropic Material Penalization) (Liu et al. 2008) at the macro-scale.

Figure 2 shows a structure with homogeneous cellular material schematically. It is a “single gray–white” design. At the macro scale, the “gray domain” is composed of homogeneous cellular material, and the “white domain” has no cellular material. And the homogeneous cellular material is assumed to be made of the base material and to have periodic microstructure free from any restriction (e.g. cellular material with square and rectangular holes, ranked laminates). In the enlarged picture of Fig. 2, the “black domain” in the unit cell of the cellular material is occupied by base material such as aluminum and alloy, and the “white domain” has no material.

Both optimum design problems at macro-structure and micro-structure scales as shown in Fig. 2 can be dealt with as classical layout designs, for which topology optimization is a powerful tool. First as shown in Fig. 2, macro domain Ω is meshed into NE elements and micro domain Y is meshed into n elements. Each element is then assigned a unique artificial volumetric relative

density value either 0 or 1 for description of material distribution, or description of the topology, that is, P_i for the i th ($i = 1, 2, \dots, NE$) element at the macro-scale, and ρ_j ($j = 1, 2, \dots, n$) for the j th element at the micro-scale. $P_i = 1$ if the i th element at the macro-scale is occupied by cellular material, $P_i = 0$ if no cellular material exists in the i th element at the macro-scale. Distribution of P_i ($i = 1, 2, \dots, NE$) describes the macro structural topology. $\rho_j = 1$ if the j th element at the micro-scale is occupied by the base material, $\rho_j = 0$ if no base material exists in the j th element at the micro-scale. Distribution of ρ_j ($j = 1, 2, \dots, n$) describes the material micro structural topology of the unit cell. Using the artificial volumetric relative density ρ_j , the mass density of the j th element at the micro-scale is $\rho_j \times \eta$, where η represents the mass density of the isotropic base material. Since an element at the macro-scale is composed of cellular material, $\rho_i^{MA} = P_i \times \rho^{PAM}$ is i th

element volumetric density, where $\rho^{PAM} = \frac{\sum_{j=1}^n \rho_j v_j^{MI}}{V^{MI}}$ denotes relative density of the cellular material. v_j^{MI} represents the area of the j th element in micro design domain and V^{MI} is the area of micro design domain. The superscript MI and MA refer to the quantities in micro design domain or the unit cell and at macro scale, respectively. The amount of base material used for constructing the structure is $\zeta \times V^{MA} = \sum_{i=1}^{NE} \rho_i^{MA} v_i^{MA} = \rho^{PAM} \times \sum_{i=1}^{NE} P_i v_i^{MA}$, where ζ is the fraction of base material on the total base material for filling up the whole macro design domain using solid material. And v_i^{MA} and V^{MA} are the areas of the i th element and the design domain at macro-scale, respectively.

3 Formulations of two-scale design optimization for maximum structural fundamental eigenfrequency

The problem of two-scale topology design for maximization of fundamental frequency of macrostructure can be formulated as follows:

$$\text{Find : } \mathbf{X} = \{\mathbf{P}, \rho\}, \tag{1}$$

$$\text{Obj : } \max \left\{ \min_{j=1, \dots, J} \left\{ \lambda_j = \omega_j^2 \right\} \right\}, \tag{2}$$

$$\text{S.t. : } \mathbf{K}\phi_j = \lambda_j \mathbf{M}\phi_j, \quad j = 1, \dots, J, \tag{3a}$$

$$\phi_j^T \mathbf{M}\phi_k = \delta_{jk}, \quad k, j = 1, \dots, J, \tag{3b}$$

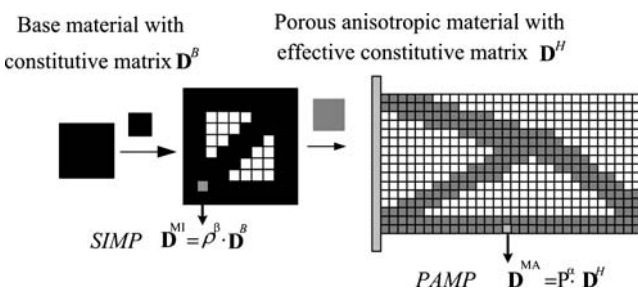


Fig. 2 A structure composed of homogeneous cellular material and penalization-based two-scale design optimization

$$\zeta = \frac{\sum_{i=1}^{NE} \rho_i^{MA} v_i^{MA}}{V^{MA}} = \frac{\rho^{PAM} \times \sum_{i=1}^{NE} P_i v_i^{MA}}{V^{MA}} \leq \bar{\zeta}, \tag{3c}$$

$$\rho^{PAM} = \frac{\sum_{l=1}^n \rho_l v_l^{MI}}{V^{MI}} = \bar{\zeta}^{MI}, \tag{3d}$$

$$0 < \underline{P} \leq P_i \leq \bar{P}, i = 1, \dots, NE, \tag{3e}$$

$$0 < \underline{\rho} \leq \rho_l \leq \bar{\rho}, l = 1, \dots, n. \tag{3f}$$

In (3), ω_j and ϕ_j denote the j th structural eigenfrequency and corresponding eigenvector, respectively. \mathbf{K} and \mathbf{M} are the positive definite symmetric stiffness and mass matrices of the macro structure. Equation (3a) is the governing equation of structural natural vibration. Equation (3b) imposes the \mathbf{M} orthonormalization condition on eigenvectors. δ_{jk} is Kronecker’s delta. In the optimization of maximum natural frequency by topology optimization, the order of the modes could change during optimization, namely so called mode switching (Ma et al. 1995; De Gournay 2006; Du and Olhoff 2007), thus J candidate frequencies are considered in the objective function (2). The eigenvalue problem is solved using the subspace iteration method (Bathe 1996).

The constraint (3c) sets the upper bound of the available base material, $\bar{\zeta} \times V^{MA}$ is prescribed base material amount, $\bar{\zeta}$ represents the fraction of prescribed base material on the total base material for filling up the whole macro design domain using solid material. The constraint (3d) specifies the relative density of the cellular material and $\bar{\zeta}^{MI}$ is the prescribed relative density of the cellular material. To avoid singularity in computation, low limit 0.001 is specified for both macro and micro volumetric material densities P and ρ .

The global stiffness matrix \mathbf{K} and mass matrix \mathbf{M} can be calculated by:

$$\mathbf{K} = \sum_{i=1}^{NE} \int_{\Omega^e} \mathbf{B}^T \times \mathbf{D}^{MA} \times \mathbf{B} d\Omega^e = \sum_{i=1}^{NE} \mathbf{K}_i^{MA}, \tag{4}$$

$$\mathbf{M} = \sum_{i=1}^{NE} \int_{\Omega^e} \rho^{MA} \times \eta \times \mathbf{N}^T \mathbf{N} d\Omega^e = \sum_{i=1}^{NE} \mathbf{M}_i^{MA}. \tag{5}$$

In these equations, \mathbf{K}_i^{MA} and \mathbf{M}_i^{MA} represent respectively the i th element stiffness and mass matrices in the

form of expanded structural global degree of freedom. \mathbf{B} and \mathbf{N} are the strain–displacement matrix and the shape function matrix at macro scale, respectively.

The two-scale optimization problem is solved by using the SLP (Sequential Linear Programming) in this paper. Explicit expression of sensitivity is important to enhance the efficiency of the derivative-based mathematical programming algorithms such as SLP.

For the examples in this paper we trace first three eigenfrequencies during the optimization process and don’t find the phenomena of switching or coincidence between fundamental frequency and other two eigenfrequencies. The curves of evolution of eigenvalues for some examples (Example 1 and Example 6) are referred to Figs. 6 and 12. Thus for all test cases presented here, the optimal fundamental eigenfrequency is unimodal and differentiable. When the k th eigenfrequency is unimodal, detailed sensitivity analysis of the two-scale optimization problem is given in the Appendix. However, multiple eigenfrequencies problem is very important in the optimization of vibrating structure. In the case of multiple eigenfrequencies, the eigenfrequencies are non-differentiable. Sensitivity analysis of multiple eigenfrequencies has been investigated extensively in many papers (see, e.g., Haug and Rousselet 1980; Seyranian et al. 1994, for an overview; Cox 1995; De Gournay 2006; Du and Olhoff 2007; and papers cited therein). We will continue to research whether the phenomenon of multiple frequencies occurs in some other boundary conditions and structural configurations for the two scale topology optimization problem. Further extensions of two scale topology optimization for multiple eigenfrequencies problem are left for future work.

4 Penalization method for topology optimization at two scales

In order to achieve clear topologies at both scales, penalization methods are applied. At micro scale, it is natural to utilize SIMP (Solid Isotropic Material with Penalty), a method commonly used in traditional structural topology optimization. Assuming modulus matrix of the base material is \mathbf{D}^B , the modulus matrix \mathbf{D}^{MI} at a point with density ρ at the micro-scale can be expressed as:

$$\mathbf{D}^{MI} = \rho^\mu \times \mathbf{D}^B. \tag{6}$$

At macro scale, since the cellular material can be anisotropic, given any porous anisotropic material with

modulus matrix \mathbf{D}^H , a point with density P has the modulus matrix \mathbf{D}^{MA} as expressed by:

$$\mathbf{D}^{MA} = P^\alpha \times \mathbf{D}^H. \tag{7}$$

By assuming $\mu > 1, \alpha > 1$, the material densities are penalized to close to either 0 or 1. Following the terminology SIMP, the macro-penalization (7) is named as PAMP (Porous Anisotropic Material with Penalty) because the penalization is applied to porous anisotropic material.

In terms of artificial volumetric relative density value P , the finite element mass matrix may be expressed as:

$$M_e = P^\xi \times M_e^* \tag{8}$$

where M_e^* represents the element mass matrix corresponding to macro element with volumetric relative density $P = 1$. $\xi = 1$ is chosen in this paper.

One of the main problems in the topology optimization with respect to eigenfrequencies or buckling loads using SIMP is the possibility of localized modes with very low values of corresponding eigenfrequencies, see, e.g., Pedersen (2000); Allaire et al. (2001). The localized modes may occur in areas with low values of the element volumetric relative densities for typical penalization values $\alpha = 3$ and $\xi = 1$. To eliminate these localized eigenmodes, many methods are presented in the field of dynamic optimization (e.g. Pedersen 2000; Cheng and Wang 2007). Based on the constraint continuity analysis approach, Cheng and Wang (2007) pointed out that the limiting value of the ratio between stiffness and mass has a great effect on the lowest eigenfrequencies when design variable P approaches to zero. For the traditional penalization values $\alpha = 3$ and $\xi = 1$, this limiting value is zero and local vibration mode could occur in areas with low values of densities.

To avoid the local vibration mode, they suggested the penalization for the element stiffness matrix:

$$\mathbf{D}^{MA} = f(P) \times \mathbf{D}^H. \tag{9}$$

And $f(P)$ should satisfy:

$$f(0) = 0, \quad f(1) = 1, \quad f(P) < P \text{ for } 0 < P < 1. \tag{10}$$

And:

$$\lim_{P \rightarrow 0} f(P)/P > 0. \tag{11}$$

After numerical experiments and elaborate analysis, a good choice is found that:

$$f(P) = 1.1P^3 - 0.2P^2 + 0.1P \tag{12}$$

which is the choice in this paper. Figure 3 shows comparison of our polynomial penalization and the traditional exponent penalization. For more discussions about the selections of penalization function, readers are referred to ref. (Cheng and Wang 2007).

In the two-scale optimization here, \mathbf{D}^H doesn't represent the constitutive matrix of isotropic base material like in traditional SIMP, but denotes the equivalent constitutive matrix of corresponding periodic cellular material. The computation of \mathbf{D}^H follows the classical homogenization procedures (Benssousan et al. 1978; Sanchez-Palencia 1980; Hassani and Hinton 1998):

$$\mathbf{D}^H = \frac{1}{|Y|} \int_Y \mathbf{D}^{MI} \times (\mathbf{I} - \mathbf{b}\mathbf{u}) dY, \tag{13}$$

$$\mathbf{D}^{MI} = \rho^\mu \times \mathbf{D}^B \tag{14}$$

where \mathbf{D}^{MI} represents constitutive matrix of the material points with density ρ at the micro-scale, \mathbf{D}^B represents the constitutive matrix of isotropic base material,

Fig. 3 Comparisons of polynomial penalization (12) and exponent penalization

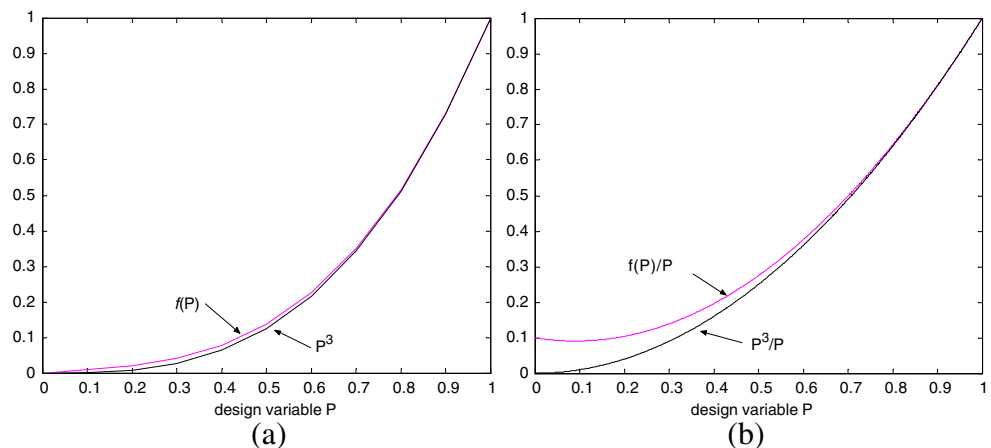
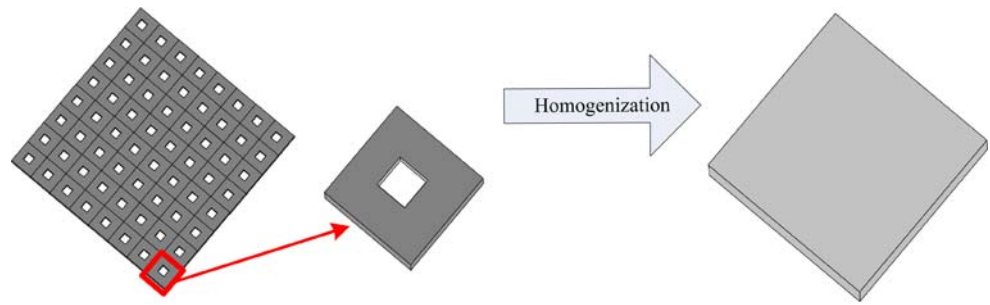


Fig. 4 Homogenization based analysis of perforated plate



\mathbf{I} (3×3) is a unit matrix in two-dimensional case, $|Y|$ is the area of a unit cell, and \mathbf{b} is the strain/displacement matrix at the micro scale. Generalized deformations \mathbf{u} of the micro-structure could be obtained from (15) and (16) below. The power μ in (14) denotes the exponent of penalization, and $\mu = 3$ is chosen in this paper:

$$\mathbf{k} \times \mathbf{u} = \int_Y \mathbf{b}^T \times \mathbf{D}^{MI} dY, \tag{15}$$

$$\mathbf{k} = \int_Y \mathbf{b}^T \times \mathbf{D}^{MI} \times \mathbf{b} dY. \tag{16}$$

With the equivalent constitutive matrix of cellular material and penalization method, the global stiffness matrix \mathbf{K} and mass matrix \mathbf{M} can now be calculated by:

$$\begin{aligned} \mathbf{K} &= \sum_{i=1}^{NE} \int_{\Omega^e} \mathbf{B}^T \times \mathbf{D}^{MA} \times \mathbf{B} d\Omega^e \\ &= \sum_{i=1}^{NE} f(P_i) \int_{\Omega^e} \mathbf{B}^T \times \mathbf{D}^H \times \mathbf{B} d\Omega^e = \sum_{i=1}^{NE} f(P_i) \mathbf{K}_i^*, \end{aligned} \tag{17}$$

$$\mathbf{M} = \sum_{i=1}^{NE} \left(P_i \times \int_{\Omega^e} \eta \times \rho^{PAM} \mathbf{N}^T \mathbf{N} d\Omega^e \right) = \sum_{i=1}^{NE} P_i \times \mathbf{M}_i^*. \tag{18}$$

In these equations, \mathbf{K}_i^* and \mathbf{M}_i^* represent respectively the i th element stiffness and mass matrices with macro element volumetric relative density $P = 1$.

5 Formulation for vibration of perforated plate

Another important type of ultra-light structure is perforated plate, which is formed by planar periodic

repetition of a homogeneous 3D microstructure, but the microstructure doesn't vary along the plate thickness direction, as shown in Fig. 4.

Considering the behavior of a thin perforated plate undergoing small deformations, it is reasonable to approximate the perforated plate as a classical anisotropic plate based on the effective properties resulting from the microstructure. The effective properties of this perforated plate can be obtained similarly based on mathematical homogenization method (Artola and Duvaut 1977; Liu et al. 1998; Bendsøe and Sigmund 2003, references therein).

The general constitutive law of the perforated plate is:

$$\mathbf{F} = \mathbf{D}^{PL} \boldsymbol{\kappa} \tag{19}$$

or in the matrix form:

$$\begin{aligned} \begin{Bmatrix} F_x \\ F_y \\ F_z \end{Bmatrix} &= \mathbf{D}^{PL} \begin{Bmatrix} -\frac{\partial^2 w}{\partial x^2} \\ \frac{\partial^2 w}{\partial y^2} \\ -2\frac{\partial^2 w}{\partial x \partial y} \end{Bmatrix} = \frac{t^3}{12} \mathbf{D}^H \begin{Bmatrix} -\frac{\partial^2 w}{\partial x^2} \\ \frac{\partial^2 w}{\partial y^2} \\ -2\frac{\partial^2 w}{\partial x \partial y} \end{Bmatrix} \\ &= \frac{t^3}{12} \begin{bmatrix} D_{11}^H & D_{12}^H & D_{13}^H \\ D_{21}^H & D_{22}^H & D_{23}^H \\ D_{31}^H & D_{32}^H & D_{33}^H \end{bmatrix} \begin{Bmatrix} -\frac{\partial^2 w}{\partial x^2} \\ \frac{\partial^2 w}{\partial y^2} \\ -2\frac{\partial^2 w}{\partial x \partial y} \end{Bmatrix} \end{aligned} \tag{20}$$

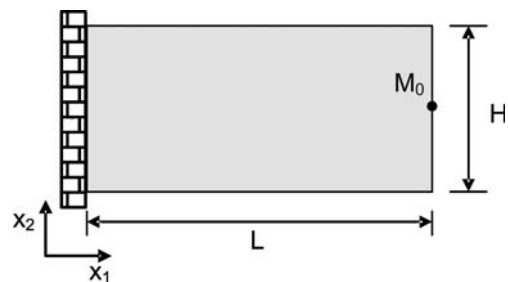


Fig. 5 Admissible design domain of beam-like 2D structure, clamped at the left wall

where t is the thickness of the thin perforated plate, F_x and F_y are normal bending moments and F_{xy} is twisting moment, κ is curvature of the thin plate, and w is the plate deflection in the direction of the z axis while the z -direction coincides with the thickness direction of the thin plate and the plate is parallel to the xy plane.

The equivalent properties \mathbf{D}^H of perforated plate can be computed in a similar way as above plane problem (Liu et al. 1998).

The global stiffness matrix \mathbf{K} and mass matrix \mathbf{M} for perforated plate can be calculated similarly. \mathbf{B}^{PL} and \mathbf{N}^{PL} are the curvature–displacement matrix and the shape function matrix of plate element at the macro scale, respectively:

$$\mathbf{K} = \sum_{i=1}^{NE} f(P_i) \int_{\Omega^e} (\mathbf{B}^{PL})^T \times \mathbf{D}^{PL} \times \mathbf{B}^{PL} d\Omega^e = \sum_{i=1}^{NE} f(P_i) \mathbf{K}_i^*, \tag{21}$$

$$\mathbf{M} = \sum_{i=1}^{NE} \left(P_i \times \int_{\Omega^e} \eta \times \rho^{PAM} (\mathbf{N}^{PL})^T \mathbf{N}^{PL} d\Omega^e \right) = \sum_{i=1}^{NE} P_i \times \mathbf{M}_i^*. \tag{22}$$

6 Numerical examples

Several numerical examples, including plane and perforated plate problems and multi domain design problem, are given in order to validate the proposed two-scale optimization method. The base material is isotropic with Young’s modulus $E = 7 \times 10^{10}$ Pa, Poisson’s ratio $\nu = 0.3$, and mass density $\eta = 2,700$ kg/m³. The mesh is 25×25 for the microstructure design domain (Eight-node element).

For suppressing the numerical instability and checkerboard patterns, the Heaviside density filtering technique (Guest et al. 2004) together with continuation method is adopted in following numerical examples. The Heaviside function for density filtering is approximated as a smooth function governed by the parameter β (Guest et al. 2004). For the two-scale optimization in this paper, the macro and micro design variables are defined in different design domains, namely macro and micro design domains. Through numerical experiments, it is recommended that different parameters β^{MA} and β^{MI} respectively for macro and micro design variables are chosen. Thus the macro

Table 1 Topological designs of macro and micro structures for varying available base material at specific micro volume fraction 40%

$\bar{\zeta}$	λ_1	Macro structure	The first mode	Micro structure	
				Cell	4×4 array
5%	67.39				
10%	156.81				
20%	487.99				
25%	593.81				

and micro densities after using the Heaviside density filtering technique become:

$$\bar{P} = 1 - e^{-\beta^{MA} \tilde{P}} + \tilde{P}e^{-\beta^{MA}}, \tag{23}$$

$$\bar{\rho} = 1 - e^{-\beta^{MI} \tilde{\rho}} + \tilde{\rho}e^{-\beta^{MI}} \tag{24}$$

where:

$$\tilde{P} = \frac{\sum_{i \in S_e^{MA}} w^{MA}(\mathbf{x}_i) P_i}{\sum_{i \in S_e^{MA}} w^{MA}(\mathbf{x}_i)}, \tag{25}$$

$$\tilde{\rho} = \frac{\sum_{j \in S_e^{MI}} w^{MI}(\mathbf{y}_j) \rho_j}{\sum_{j \in S_e^{MI}} w^{MI}(\mathbf{y}_j)}. \tag{26}$$

\bar{P} and $\bar{\rho}$ are the filtered design variables. The weighting functions $w^{MA}(\mathbf{x}_i)$ and $w^{MI}(\mathbf{y}_i)$ are defined by:

$$w^{MA}(\mathbf{x}_i) = \begin{cases} (R - \|\mathbf{x}_i - \mathbf{x}_e\|)/R, & \text{if } \mathbf{x}_i \in S_e^{MA} \\ 0, & \text{otherwise} \end{cases}, \tag{27}$$

$$w^{MI}(\mathbf{y}_j) = \begin{cases} (r - \|\mathbf{y}_j - \mathbf{y}_e\|)/r, & \text{if } \mathbf{y}_j \in S_e^{MI} \\ 0, & \text{otherwise} \end{cases}. \tag{28}$$

R is the given filter radius in the macro design domain, and r is the given filter radius in the micro design domain. The primary role of the filter radius is to identify the elements that influence the relative density of element e . For example, in the macro design domain we draw a circle of radius R centered at the center of element e , thus generate the circular sub-domain S_e^{MA} . Elements with centers located inside S_e^{MA} contribute to the computation of relative density of element e in the macro domain. Similarly the sub-domains S_e^{MI} is also specified by the elements that have centers within the given filter radius r of the center of the element e in the micro design domain. \mathbf{x}_i and \mathbf{y}_j denote the spatial (center) locations of the element i in the macro design domain and element j in the micro design domain, respectively. The Heaviside density filter is employed using a continuation approach where low values of β^{MA} and β^{MI} are used in the start, e.g. $\beta^{MA} = 0$ and $\beta^{MI} = 0$, their values are gradually increased until the satisfactory results are obtained if lots of intermediate densities exist in the converged topology. However, when the two parameters β^{MA} and β^{MI} are increased uniformly clear topologies of macro and micro structures are hard to be obtained simultaneously. Through

Table 2 Topological designs of macro and micro structures with varying micro volume at available base material amount 20%

$\bar{\zeta}^{MI}$	λ_1	Macro structure	The first mode	Micro structure	
				Cell	4x4 array
30%	435.81				
40%	487.99				
60%	508.96				
100%	558.02				

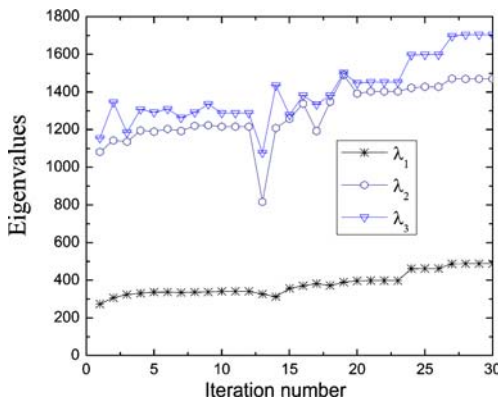


Fig. 6 Iteration histories of the first three eigenvalues for the process leading to the topology designs in fourth row of Table 1 with available base material amount $\bar{\zeta} = 20\%$ and specific micro volume fraction $\bar{\zeta}^{MI} = 40\%$

numerical experiments, it is found that convergence is relatively stable when the two parameters β^{MA} and β^{MI} are changed independently, e.g. $\beta^{MA} = \beta^{MA} + 1$ and $\beta^{MI} = \beta^{MI} + 4$ after one converged optimization. Meanwhile, in Heaviside density filter using continuation method it is normally recommended to start with large filter radiuses and gradually decrease them. In our numerical experiments, the initial values of the radiuses R and r are respectively about three or four times larger than the lengths of the macro and micro elements, and the radiuses R and r approximately equal the lengths of the macro and micro elements respectively when two-scale optimization is finished.

Example 1 The first example is topological design of a beam-like macrostructure modeled by 2D plane elements. As shown in Fig. 5, the admissible macro design domain is an 80×50 m rectangle with clamped support at the left wall and a concentrated mass $M_0 =$

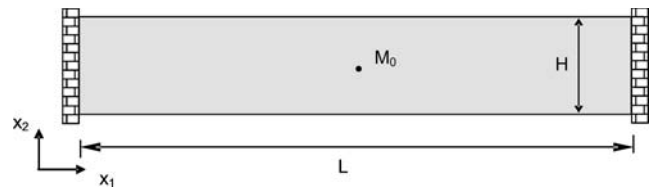


Fig. 7 Admissible design domain of beam-like 2D structure with two clamped ends

216,000 kg at the center of the right side. Finite element model of 48×30 eight-node elements is utilized for dynamic analysis and optimum design. The design objective is to maximize the fundamental eigenfrequency for different prescribed base material volume fraction and different prescribed micro material volume fraction. Table 1 lists topological designs of macro and micro structures with variation of available base material at a specific micro volume fraction $\bar{\zeta}^{MI} = 40\%$. Table 2 lists topological designs of macro and micro structures with varying specific micro volume fraction for available base material amount $\bar{\zeta} = 20\%$.

The initial values for macro design variable are uniform with value 0.5. The initial value for micro design variable is proportional to its distance from the center of the unit cell domain.

It can be seen from Table 1 that for specific constant micro volume fraction 40%, the fundamental frequency of the macro structure rises and the configurations of macro and micro structures change correspondingly with the increase of available base material. The configurations of the macro structure change from 2-bar like structure to more complicated structure when the base material increases from 5% to 25%. For the base material amount 25% the material microstructure is like Kagome cell, which is believed a very good microstructure. Iteration histories of the first three eigenvalues for

Table 3 Topological design of macro and micro structure

$\bar{\zeta}$	$\bar{\zeta}^{MI}$	λ_1	Macro structure	Micro structure	
				Cell	4×4 array
20%	40%	40822.96			
The first mode of the macro structure					

Table 4 Topological design of single micro-scale optimization

$\bar{\zeta}^{MI}$	λ_1	The first mode of Macro structure	Micro structure	
			Cell	4x4 array
20%	15674.20			
30%	23400.65			
40%	36221.73			

the case of the fourth row in Table 1 are given in Fig. 6, which shows the fundamental eigenfrequency always remains unimodal during optimization process for this case. Similarly, we checked that the optimal fundamental eigenfrequency is unimodal and differentiable for all test cases presented in this paper.

In Table 2 the six columns list the specific micro volume fraction, the fundamental eigenvalue of optimum macro structure, its topology and fundamental vibration mode, the optimum topology of the unit cell and the optimum material microstructure. For all examples, the amount of available base material is 20%. Because the amount of available base material is fixed, the volume fraction of cellular material in macro design domain decreases as the specific micro volume fraction of base material at the micro scale increases. It can be seen that the fundamental eigenfrequency increases as the specific micro volume fraction of base material at the micro scale increases. In the extreme case when the specific micro volume fraction is 100%, which means that solid material without porosity is used to construct the structure, the two-scale optimization degenerates to the traditional macro structure topology optimization. This extreme case gives the highest fundamental frequency. This interesting observation somehow is unexpected because it is often claimed in literatures that ultralight material such as truss-like material has high stiffness–weight ratio. However, structures made of porous material usually undertake other functions such as active cooling, noise damping and thermal insulation. Though the present two-scale optimization method gives optimum topology of macro structure and micro structure simultaneously with the objective of maximum fundamental frequency, this optimum ultra-

light structure provides a good initial configuration for further considering multifunctional applications.

Example 2 In the second example as shown in Fig. 7, the admissible macro design domain is a 14×2 m rectangle with fixed support boundaries at the left and right sides and a concentrated mass $M_0 = 1,512$ kg at the center of the design domain. Finite element models of 140×20 eight-node elements are utilized. The design objective is to maximize the fundamental eigenfrequency for prescribed base material volume fraction $\bar{\zeta} = 20\%$ and prescribed micro material volume fraction $\bar{\zeta}^{MI} = 40\%$. The optimum unit cell in the two-scale optimization is a Kagome cell, which is believed a good configuration for the future multifunctional application of cellular materials.

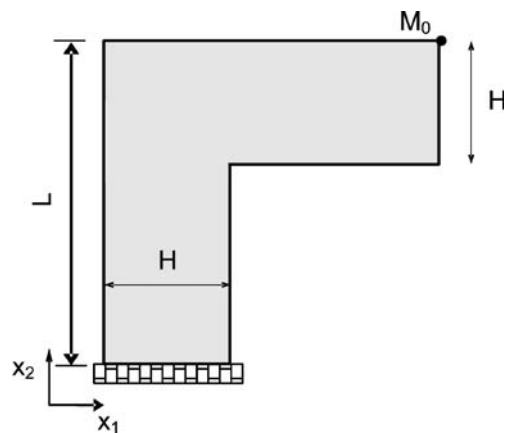

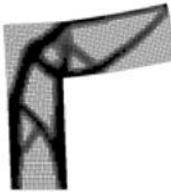




Fig. 8 Admissible design domain of L-Shape 2D structure

Table 5 Topological design of macro and micro structure

$\bar{\zeta}$	$\bar{\zeta}^{MI}$	λ_1	Macro structure	The first mode	Micro structure	
					Cell	4x4 array
16%	40%	66965.18				

6.1 Comparisons between two-scale optimization and single micro-scale optimization

In the two-scale optimization method above, macro and micro densities are introduced as independent design variables for macro structure and material microstructure. In order to illustrate the advantages of the two-scale optimization method, we compare the optimum designs from the two-scale optimization and the single micro-scale optimization. In the single micro-scale optimization, only the material microstructure needs to be designed and the macrostructure don't change in the optimization. It means that the macro design domain is filled up with the uniform cellular material everywhere. The single micro-scale optimization for maximizing the fundamental frequency is formulated as:

Find : $\mathbf{X} = \{\rho\}$
 Obj : $\max \left\{ \min_{j=1, \dots, J} \left\{ \lambda_j = \omega_j^2 \right\} \right\}$
 S.t. : $\mathbf{K}\phi_j = \lambda_j \mathbf{M}\phi_j, j = 1, \dots, J$
 $\phi_j^T \mathbf{M}\phi_k = \delta_{jk}, k, j = 1, \dots, J$
 $\rho^{PAM} = \frac{\int_Y \rho^{MI} dY}{V^{MI}} = \bar{\zeta}^{MI}$
 $0 < \underline{\rho} \leq \rho_l \leq \bar{\rho}, l = 1, \dots, n$ (29)

where micro densities are introduced as design variables for material microstructure topology optimization. The macro densities $P_i = 1 (i = 1, \dots, NE)$ are fixed.

Now let us apply the formulation (29) to the example in Fig. 7. The resulting optimum micro structure designs are given in Table 4.

Comparing the results in Tables 3 and 4, the fundamental eigenvalue 40,822.96 obtained by two-scale optimization in Table 3 is higher than the fundamental eigenvalue 36,221.73 obtained by single micro-scale optimization in the fourth row of Table 4 for same micro volume fraction $\bar{\zeta}^{MI} = 40\%$. Furthermore, base material amount $\bar{\zeta}$ used in two-scale optimization is 20% in Table 3, but 40% base material is used in single micro-scale optimization in the fourth row of Table 4 for same micro volume fraction $\bar{\zeta}^{MI} = 40\%$. When the actually used base material amount is also 20% for single micro-scale optimization shown in the second line of Table 4, the fundamental eigenvalue is 15,674.20 which is much lower than the fundamental eigenvalue 40,822.96 obtained by two-scale optimization for same amount of base material in Table 3. Thus the two-scale design optimization realizes the optimal distribution of base material at macro and micro scales and obtains the

Fig. 9 a and b Admissible design domains of 2D plane structure with different locations of concentrated masses

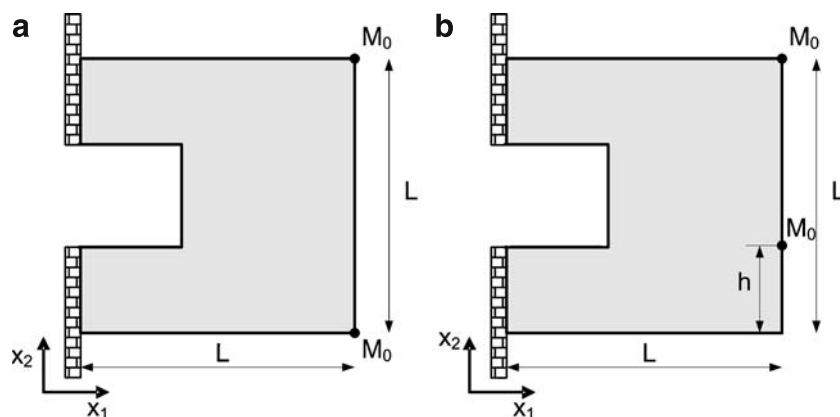


Table 6 Topological design of macro and micro structures considering different locations of concentrated masses: (a) the case of Fig. 9a, (b) the case of Fig. 9b

(a): the case of the Fig. 9(a)

$\bar{\zeta}$	$\overline{\zeta}^{MI}$	λ_1	Macro structure	The first mode	Micro structure	
					Cell	4x4 array
25%	40%	222886.19				

(b): the case of the Fig. 9(b)

$\bar{\zeta}$	$\overline{\zeta}^{MI}$	λ_1	Macro structure	The first mode	Micro structure	
					Cell	4x4 array
25%	40%	323886.92				

optimal configurations of macro and micro structures simultaneously.

Example 3 The third example is the topological design of an L-shape structure with fixed support boundaries at its bottom. As shown in Fig. 8, the dimensions of L-shape admissible design domain are $H = 0.5$ m, $L = 1.5$ m and a concentrated mass $M_0 = 67.5$ kg at the top of the right-hand side. The finite element models of 2,000 eight-node elements are utilized. The design objective is to maximize the fundamental eigenfrequency for prescribed base material volume fraction 16% and prescribed micro material volume fraction 40%.

Example 3 gives the effects of different macro design domains and boundary conditions on the configurations of macrostructure and microstructure. In this example, it can be observed that the microstructure is anisotropic under complicated conditions. It should be emphasized that the microstructures are connected because the microstructures are arranged periodically, shown in the last column of Table 5.

Example 4 As shown in Fig. 9a and b, the design domain is a 3.0×3.0 m square area with a 1.0×1.0 m square break in the left side and fixed at the left side.

The finite element models of 3,200 eight-node elements are utilized. The design objective is to maximize the fundamental eigenfrequency for prescribed base material volume fraction 25% and prescribed micro material volume fraction 40%. Two concentrated masses with same magnitude $M_0 = 432$ kg are attached to different location of the design domain, as shown in Fig. 9a and b. In Fig. 9b, $h = 1.05$ m.

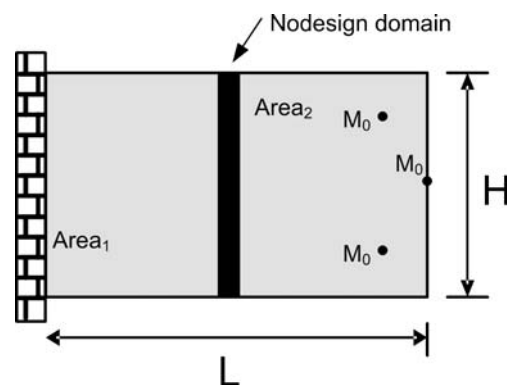

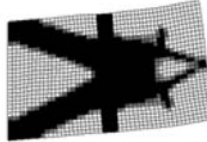

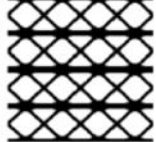

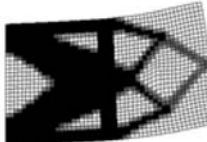

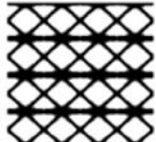


Fig. 10 Admissible design domain of 2-D structure with two design domains and a nondesign area

Table 7 Topological design of macro and micro structures with multi design domains and a nondesign area

$\bar{\zeta}_1$	$\bar{\zeta}_2$	$\bar{\zeta}^{MI}$	λ_1	Macro structure	The first mode	Micro structure	
						Cell	4×4 array
9.2%	9.2%	40%	1147.84				
13.8%	4.6%	40%	1458.89				

Different locations of concentrated masses affect the optimal configurations of macro and micro structures (Table 6). When the locations of two concentrated masses are symmetric shown in Fig. 9a, the macro and micro structures have symmetry. When this symmetry is violated, the optimal configurations of macro and micro structures also lose the symmetry in Fig. 9b.

Example 5 Multi-domain optimization. A multi-domain topology optimization technique is developed in traditional topology optimization by Ma et al. (2006). This example illustrates how the two-scale optimization method can be applied to the multi-domain optimization problem. Figure 10 depicts a structure (30×50 m) whose optimal topology is sought in two design domains, respectively denoted by “Area₁ and Area₂”, and the structure has a bar at the center of the domain referred to as a nondesign domain (30×4 m). The

structure needs to support three lumped masses with same magnitude $M_0 = 27,000$ kg distributed in the right design domain “Area₂”, as shown in Fig. 10. In this example, the objective is to maximize the fundamental eigenfrequency of the structure so as to limit its vibration response under certain operating conditions. It is assumed that the total amount of the available base material is 18.4% and the relative density of the microstructure is 40%. Table 7 lists two cases for the design which have different amount of base material in two design domains. In first case, the base material of the total amount 18.4% is assigned equally to the Area₁ and Area₂. In the second case, the base material of 13.8% and 4.6% is assigned to the Area₁ and Area₂, respectively. In these two cases, the relative density of the microstructure is given as 40%. It is assumed that the structures in the two design domains and the nondesign domain are made of same cellular material with uniform microstructure.

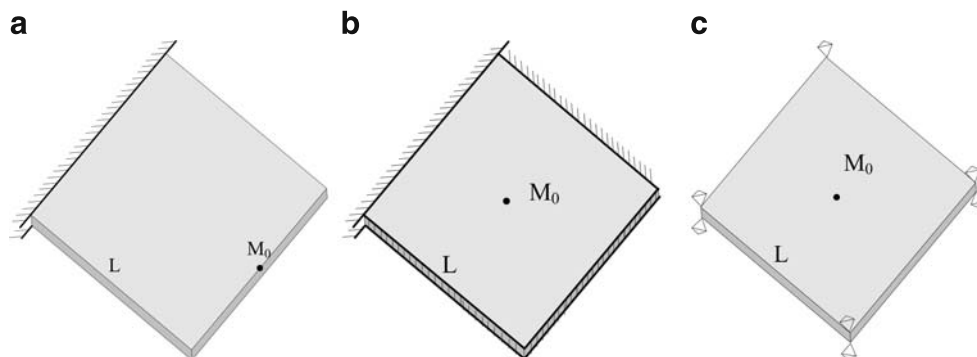


Fig. 11 Admissible design domains of perforated plate with different boundary conditions: **a** One edge clamped, other edges free, and concentrated mass $M_0 = 1.8$ kg attached at the midpoint of the edge opposite to the clamped one. **b** Four edges

clamped and concentrated mass $M_0 = 0.54$ kg at the center. **c** Simple supports at four corners and concentrated mass $M_0 = 1.8$ kg at the center of the structure

When base material of total 18.4% amount is assigned to different domains, different assignments can result in different configurations at the macro scale. However, because the constraint of microstructural relative density dose not change the configurations of the microstructures have only slight variation. Thus, when different domains have different functions in the structure made of ultralight material, the two-scale optimization method presented here can be used to realize the multidomain design problem at both macro and micro scales.

Example 6 Following the two-scale optimization formulation, optimal topology design of thin perforated

plate at the macro scale and optimal configuration of microstructure at the micro scale can be obtained simultaneously.

Three perforated plates, see Fig. 11a–c, are studied here. They have the same admissible design domain (1.0×1.0 m), but three different boundary conditions and attached concentrated masses. The detailed descriptions of the boundary conditions are given in the captions of Fig. 11. The thickness of the plate is assumed as 0.01 m.

Table 8 lists topological design of macro and micro structures at specific micro volume fraction $\bar{\zeta}^{MI} = 40\%$ and available base material amount $\bar{\zeta} = 20\%$. The

Table 8 Topological design of macro and micro structures for perforated plates only with planar periodicity (a) one edge clamped, other edges free, (b) four edges clamped, and (c) simple supports at four corners

(a) One edge clamped, other edges free						
$\bar{\zeta}$	$\bar{\zeta}^{MI}$	λ_1	Macro structure	The first mode	Micro structure	
					Cell	4×4 array
20%	40%	1254.48				
(b) Four edges clamped						
$\bar{\zeta}$	$\bar{\zeta}^{MI}$	λ_1	Macro structure	The first mode	Micro structure	
					Cell	4×4 array
20%	40%	63547.57				
(c) Simple supports at four corners						
$\bar{\zeta}$	$\bar{\zeta}^{MI}$	λ_1	Macro structure	The first mode	Micro structure	
					Cell	4×4 array
20%	40%	6483.67				

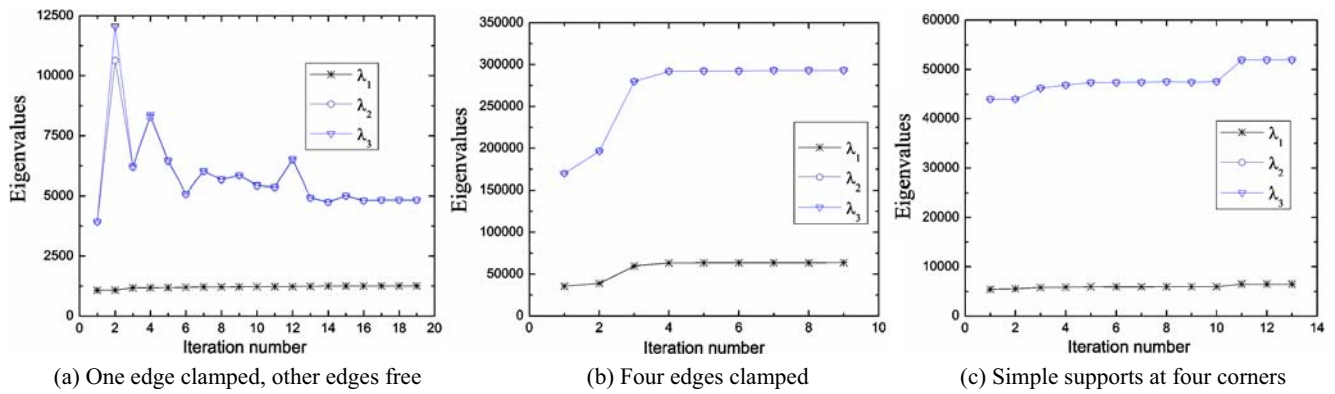


Fig. 12 Iteration histories of the first three eigenvalues for the process leading to the topology designs in Table 8: one edge clamped, other edges free (a), four edges clamped (b), simple supports at four corners (c)

resulting optimum macro and micro topologies agree with our common sense very well. It is clear in Fig. 12 that the fundamental eigenfrequency always remains unimodal during the optimization process.

7 Concluding remarks

The present paper studies optimum structural and material topology design for maximum fundamental frequency. To meet today's manufacturing limitation, the present paper assumes homogeneous material microstructure at macro scale. The two-scale design optimization formulation and numerical treatment for maximum frequency design are presented. It realizes the optimal distribution of base material at macro and micro scales and obtains the optimal configurations of macro and micro structures simultaneously. These novel configurations provide the guideline for further study on structure design of cellular material in vibration environments.

The results of two-scale topology optimization in this paper give good mechanical properties and these good mechanical properties are the basis of further multifunctional applications of the structure made of cellular material. And the optimum microstructure provides a good initial configuration for the future multifunctional application of cellular materials. Additionally, different microstructures are required for different structures under different conditions when we use macro-homogeneous material for structures. Two-scale design optimization of structural macro-topology and material micro-topology is an important tool for ultra-light structure design.

Furthermore, it will be an interesting and challenging work to extend this two-scale optimization method to more realistic applications, e.g. including mechanical

failure in constraints and multifunctional performances such as active or passive heat transfer, vibration isolation and mechanical material failure into one system.

Acknowledgements The financial support for this research was provided by the National Natural Science Foundation of China (no. 90816025, 50878038), National Creative Research Team Program of China (no. 10721062), National Basic Research Program of China through Grant No. 2006CB601205, the start funds for introducing researchers of DUT and DCAMM of Denmark. These supports are gratefully appreciated. We also acknowledge the China Scholarship Council (CSC) for partial support of Bin Niu, who was awarded the CSC Scholarship.

Appendix

Sensitivity analysis of a unimodal structural frequency with respect to macro density and micro density design variables:

If the k th eigenfrequency is unimodal, then the corresponding eigenvector ϕ_k will be unique (up to a factor) and differentiable with respect to the artificial design variables P and ρ .

The derivative of k th eigenvalue λ_k with respect to the macro design variables P_j is expressed as:

$$\frac{\partial \lambda_k}{\partial P_j} = \phi_k^T \left(\frac{\partial \mathbf{K}}{\partial P_j} - \lambda_k \frac{\partial \mathbf{M}}{\partial P_j} \right) \phi_k, \quad j = 1, \dots, NE. \quad (30)$$

The derivatives of the matrices \mathbf{K} and \mathbf{M} can be calculated explicitly from the material models in Section 4 and 5. Considering, e.g., the material model in (21) and (22):

$$\frac{\partial \mathbf{K}}{\partial P_j} = f'(P_j) K_j^*, \quad (31)$$

$$\frac{\partial \mathbf{M}}{\partial P_j} = M_j^*. \quad (32)$$

Sensitivity of the objective λ_k with respect to micro design variable ρ_j :

$$\frac{\partial \lambda_k}{\partial \rho_j} = \phi_k^T \left(\frac{\partial \mathbf{K}}{\partial \rho_j} - \lambda_k \frac{\partial \mathbf{M}}{\partial \rho_j} \right) \phi_k, \tag{33}$$

$$\begin{aligned} \frac{\partial \mathbf{K}}{\partial \rho_j} &= \frac{\partial \left[\sum_{i=1}^{NE} (f(P_i) \times \mathbf{K}_i^*) \right]}{\partial \rho_j} \\ &= \frac{\partial \left[\sum_{i=1}^{NE} \left(f(P_i) \times \int_{\Omega^e} \mathbf{B}^T \times \mathbf{D}^H \times \mathbf{B} d\Omega^e \right) \right]}{\partial \rho_j} \\ &= \sum_{i=1}^{NE} \left(f(P_i) \times \int_{\Omega^e} \mathbf{B}^T \times \frac{\partial \mathbf{D}^H}{\partial \rho_j} \times \mathbf{B} d\Omega^e \right) \end{aligned} \tag{34}$$

Where: $\frac{\partial \mathbf{D}^H}{\partial \rho_j} = \frac{1}{|Y|} \int_Y (\mathbf{I} - \varepsilon_y^T(\mathbf{u})) \frac{\partial \mathbf{D}^{MI}}{\partial \rho_j} (\mathbf{I} - \varepsilon_y(\mathbf{u})) dY,$

$$\begin{aligned} \frac{\partial M}{\partial \rho_j} &= \frac{\partial \left[\sum_{i=1}^{NE} \left(P_i \times \int_{\Omega^e} \eta \times \rho^{PAM} \times \mathbf{N}^T \mathbf{N} d\Omega^e \right) \right]}{\partial \rho_j} \\ &= \sum_{i=1}^{NE} \left(P_i \times \int_{\Omega^e} \eta \times \frac{\partial \rho^{PAM}}{\partial \rho_j} \times \mathbf{N}^T \mathbf{N} d\Omega^e \right) \end{aligned} \tag{35}$$

Where: $\frac{\partial \rho^{PAM}}{\partial \rho_j} = \frac{\partial \left(\frac{f \rho dY}{V^{MI}} \right)}{\partial \rho_j} = \frac{\partial \sum_{j=1}^n \rho_j A^j}{\partial \rho_j} \frac{1}{V^{MI}} = \frac{A^j}{V^{MI}}.$

References

Allaire G (2002) Shape optimization by the homogenization method. Springer, New York
 Allaire G, Jouve F (2005) A level-set method for vibration and multiple loads structural optimization. *Comput Methods Appl Mech Eng* 194(30–33):3269–3290
 Allaire G, Aubry S, Jouve F (2001) Eigenfrequency optimization in optimal design. *Comput Methods Appl Mech Eng* 190(28):3565–3579
 Allaire G, Jouve F, Toader AM (2002) A level-set method for shape optimization. *C R Acad Sci Ser 1 Math* 334(12):1125–1130
 Artola M, Duvaut G (1977) Homogeneization of a reinforced plate. *C R Hebd Seances Acad Sci Ser A Sci Math* 284(12):707–710
 Ashby MF, Evans AG, Fleck NA et al (2000) Metal foams: a design guide. Butterworth-Heinemann, Boston
 Banerjee S, Bhaskar A (2005) Free vibration of cellular structures using continuum modes. *J Sound Vib* 287(1–2):77–100

Bathe KJ (1996) Finite element procedures. Englewood Cliffs, Prentice-Hall, NJ
 Bendsøe MP (1989) Optimal shape design as a material distribution problem. *Struct Optim* 1:193–202
 Bendsøe MP, Kikuchi N (1988) Generating optimal topologies in structural design using a homogenization method. *Comput Methods Appl Mech Eng* 71(2):197–224
 Bendsøe MP, Sigmund O (2003) Topology optimization: theory, methods and applications. Springer, Berlin
 Benssousan A, Lions JL, Papanicoulau G (1978) Asymptotic analysis for periodic structures. North Holland, Amsterdam
 Borst Rd (2008) Challenges in computational materials science: multiple scales, multi-physics and evolving discontinuities. *Comput Mater Sci* 43(1):1–15
 Brittain ST, Sugimura Y, Schueller OJA et al (2001) Fabrication and mechanical performance of a mesoscale space-filling truss system. *J Microelectromechanical Syst* 10(1):113–120
 Cheng G, Olhoff N (1981) An investigation concerning optimal design of solid elastic plates. *Int J Solids Struct* 17(3):305–323
 Cheng G, Wang B (2007) Constraint continuity analysis approach to structural topology optimization with frequency objective/constraints. In: Kwak BM et al (eds) *Proceeding of the 7th world congress of structural and multidisciplinary optimization*, Seoul, Korea, pp 2072
 Cherkhaev A (2000) Variational methods for structural optimization. Springer, New York
 Cochran JK, Lee KJ, McDowell D et al (2002) Multifunctional metallic honeycombs by thermal chemical processing. In: Ghosh A et al (eds) *Processing and properties of light-weight cellular metals and structures*. TMS, Warrendale, PA, pp 127
 Cox SJ (1995) The generalized gradient at a multiple eigenvalue. *J Funct Anal* 133(1):30–40
 De Gournay F (2006) Velocity extension for the level-set method and multiple eigenvalues in shape optimization. *SIAM J Control Optim* 45(1):343–367
 Deshpande VS, Fleck NA, Ashby MF (2001) Effective properties of the octet-truss lattice material. *J Mech Phys Solids* 49:1747–1769
 Diaz AR, Kikuchi N (1992) Solutions to shape and topology eigenvalue optimization problems using a homogenization method. *Int J Numer Methods Eng* 35(12):1487–1502
 Du JB, Olhoff N (2007) Topological design of freely vibrating continuum structures for maximum values of simple and multiple eigenfrequencies and frequency gaps. *Struct Multidisc Optim* 34(2):91–110
 Eschenauer H, Olhoff N (2001) Topology optimization of continuum structures: a review. *Appl Mech Rev* 54(4):331–389
 Evans AG, Hutchinson JW, Fleck NA et al (2001) The topological design of multifunctional cellular metals. *Prog Mater Sci* 46(3–4):309–327
 Gibson LJ, Ashby MF (1997) Cellular solids: structure and properties. Cambridge University Press, Cambridge
 Guest JK, Prevost JH, Belytschko T (2004) Achieving minimum length scale in topology optimization using nodal design variables and projection functions. *Int J Numer Methods Eng* 61(2):238–254
 Hassani B, Hinton E (1998) A review of homogenization and topology optimization I, II. *Comput Struct* 69(6):707–738
 Haug EJ, Rousselet B (1980) Design sensitivity analysis in structural mechanics. II. Eigenvalue variations. *J Struct Mech* 8(8):161–186
 Hayes AM, Wang AJ, Dempsey BM et al (2004) Mechanics of linear cellular alloys. *Mech Mater* 36(8):691–713

- Hohe J, Becker W (2002) Effective stress–strain relations for two-dimensional cellular sandwich cores: homogenization, material models, and properties. *Appl Mech Rev* 55(1): 61–87
- Hyun S, Torquato S (2002) Optimal and manufacturable two-dimensional, Kagome-like cellular solids. *J Mater Res* 17:137–144
- Jensen JS, Pedersen NL (2006) On maximal eigenfrequency separation in two-material structures: the 1D and 2D scalar cases. *J Sound Vib* 289(4–5):967–986
- Kooistra GW, Deshpande VS, Wadley HNG (2004) Compressive behavior of age hardenable tetrahedral lattice truss structures made from aluminium. *Acta Mater* 52(14):4229–4237
- Krog LA, Olhoff N (1999) Optimum topology and reinforcement design of disk and plate structures with multiple stiffness and eigenfrequency objectives. *Comput Struct* 72(4): 535–563
- Lipperman F, Fuchs MB, Ryvkin M (2008) Stress localization and strength optimization of frame material with periodic microstructure. *Comput Methods Appl Mech Eng* 197 (45–48):4016–4026
- Liu L, Yan J, Cheng G (2008) Optimum structure with homogeneous optimum truss-like material. *Comput Struct* 86 (13–14):1417–1425
- Liu S, Cheng G, Gu Y et al (1998) Homogenization-based method for bending analysis of perforated plate. *Acta Mech Solida Sinica* 11(2):172–179
- Ma ZD, Kikuchi N, Cheng HC (1995) Topological design for vibrating structures. *Comput Methods Appl Mech Eng* 121 (1–4):259–280
- Ma ZD, Kikuchi N, Pierre C et al (2006) Multidomain topology optimization for structural and material designs. *J Appl Mech* 73(4):565–573
- Pedersen NL (2000) Maximization of eigenvalues using topology optimization. *Struct Multidisc Optim* 20(1):2–11
- Rodrigues H, Guedes JM, Bendsoe MP (2002) Hierarchical optimization of material and structure. *Struct Multidisc Optim* 24(1):1–10
- Rozvany G, Zhou M, Birker T (1992) Generalized shape optimization without homogenization. *Struct Optim* 4:250–252
- Sanchez-Palencia E (1980) Non-homogeneous media and vibration theory, lecture notes in physics, vol 127. Springer, Berlin
- Seyranian AP, Lund E, Olhoff N (1994) Multiple eigenvalues in structural optimization problems. *Struct Optim* 8(4):207–227
- Sigmund O (1995) Tailoring materials with prescribed elastic properties. *Mech Mater* 20(4):351–368
- Sigmund O, Jensen JS (2003) Systematic design of phononic band-gap materials and structures by topology optimization. *Philos Trans R Soc Lond Ser A Math Phys Sci* 361 (1806):1001–1019
- Tartar L (2000) An introduction to the homogenization method in optimal design in optimal shape design (Troia, 1998). In: Cellina A, Ornelas A (eds) *Lecture notes in mathematics*, vol 1740. Springer, Berlin, pp 47–156
- Wallach JC, Gibson LJ (2001) Mechanical behavior of a three-dimensional truss material. *Int J Solids Struct* 38:7181–7196
- Wang XL, Stronge WJ (1999) Micropolar theory for two-dimensional stresses in elastic honeycomb. *Proc R Soc Lond A Math Phys Sci* 455(1986):2091–2116
- Wang MY, Wang X, Guo D (2003) A level set method for structural topology optimization. *Comput Methods Appl Mech Eng* 192(1–2):227–246
- Xie YM, Steven GP (1993) A simple evolutionary procedure for structural optimization. *Comput Struct* 49(5):885–896
- Xue Z, Hutchinson JW (2003) Preliminary assessment of sandwich plates subject to blast loads. *Int J Mech Sci* 45:687–705
- Yan J, Cheng G, Liu S et al (2006) Comparison of prediction on effective elastic property and shape optimization of truss material with periodic microstructure. *Int J Mech Sci* 48(4): 400–413